



Mar, Nang Seng Siri and Fookes, Clinton and Prasad, K.D.V. Yarlagadda (2010)  
*Automatic Solder Joint Defect Classification using the Log-Gabor Filter.*  
Advanced Materials Research, vol. 97-101. pp. 2940-2943.

© Copyright 2010 Trans Tech Publications Ltd.

# Automatic Solder Joint Defect Classification using the Log-Gabor Filter

Nang Seng Siri Mar<sup>a</sup>, Dr. Clinton Fookes<sup>b</sup>, Prof. Prasad K.D.V.Yarlagadda<sup>c</sup>

School of Engineering Systems

Queensland University of Technology

2, George Street, Brisbane QLD 4001, AUSTRALIA

<sup>a</sup>[marn@qut.edu.au](mailto:marn@qut.edu.au), <sup>b</sup>[c.fookes@qut.edu.au](mailto:c.fookes@qut.edu.au), <sup>c</sup>[y.prasad@qut.edu.au](mailto:y.prasad@qut.edu.au)

**Keywords:** Automatic PCB inspection, Feature extraction, Classification, Log-Gabor filter, Mahalanobis Cosine Distance.

**Abstract.** This paper proposes the validity of a Gabor filter bank for feature extraction of solder joint images on Printed Circuit Boards (PCBs). A distance measure based on the Mahalanobis Cosine metric is also presented for classification of five different types of solder joints. From the experimental results, this methodology achieved high accuracy and a well generalised performance. This can be an effective method to reduce cost and improve quality in the production of PCBs in the manufacturing industry.

## Introduction

Assembly of Printed Circuit Boards (PCBs) using Surface Mount Technology (SMT) has been widely used in the electronics industry recently [1] and the quality of the solder joint is critical to the quality of PCBs. Automatic Optical Inspection (AOI) of solder joints has become an important issue for quality control in PCB assembly as AOI has the enormous potential of completely automating human visual inspection procedures. The aim of these inspection procedures is to detect and locate any potential solder joint defects which will break down the functions of the final PCB products. Common solder joint defects which are of interest include: excess solder, less solder, no solder, and bridge solder joints [2]. Many research techniques have been developed to recognize faulty solder joints. Kim *et al.* [3] used active lighting and a Multi Layer Perceptron network to classify 2D features and a Bayes classifier to classify 3D features. Other techniques include Artificial Neural Network (ANN) ensembles [4] which combine a genetic algorithm and AdaBoost algorithm to correct a former trained ANN's errors. Jiang *et al.* [2] introduced a simpler method to identify the positions of the solder joint and a tree structure classifier to categorise the defect of the solder joint. This methodology does not require special lighting or special equipment to capture the PCB image. Accianni *et al.* [5] extracted Wavelet coefficients and geometric parameters of the images and used a neural network system to characterise the solder joint defects on PCBs assembled in SMT. To improve the recognition rate, Ong *et al.* [6] combined the orthogonal view and the oblique view at the pixel level with direct input to the (ANN) for processing.

Although many methods have been developed in this area, these methods need a complex system of image acquisition. It is also important to select the right classification method to improve the detection rate. This paper introduces a new technique for solder joint defect classification using the Gabor filter which has been demonstrated to achieve a high recognition rate and is resistant to misalignment [7]. This filter has also found favour in many image processing fields due to its desirable characteristics of spatial locality and orientation selectivity. The next section of this paper introduces the Log-Gabor method and the Mahalanobis Cosine Distance. The remaining sections present the experimental results, discussion and conclusion.

## Gabor and Log-Gabor Filter

An important property of the Gabor filter is that it has optimal localisation properties in both the spatial and frequency domain [8]. A two-dimensional Gabor filter consists of a sinusoidal plane of the particular frequency and orientation modulated by a two dimensional Gaussian envelope. The two main components of a Gabor filter are the complex sinusoidal carrier  $s(x)$  and the Gaussian envelope  $\omega_r(x)$ . These components are expressed as,

$$s(x) = \exp\{2\pi j k^T x\}, \quad (1)$$

where  $k = [\nu_0 \nu_0 \omega_0]$  defines the spatial frequency of the complex valued plane wave and,

$$\omega_r(x) = K \exp\{-\pi(\alpha^T [R_\theta(x - x_0)])^2\}, \quad (2)$$

where  $K$  is a scaling factor,  $\alpha = [\sigma_1^2 \sigma_2^2 \dots \sigma_N^2]^T$  the variance of the Gaussian and  $x_0$  is the spatial coordinates of the peak. The  $R_\theta$  is a rotation of the Gaussian about its centre.

The Gabor filter bank is a well known technique to determine a feature domain for the representation of an image. A Gabor filter bank can be designed by varying the spatial frequency and orientation of a Gabor filter which mimics a band-pass filter. However, a Gabor filter can be designed for a bandwidth of 1 octave maximum with a small DC component in the filter. To overcome this limitation, Field [9] proposes the Log-Gabor filter. A Log-Gabor filter has no DC component and can be constructed with any arbitrary bandwidth. The frequency response of a Log-Gabor filter is defined as,

$$\Phi(\omega) = \exp - \frac{\ln(\omega / \omega_0)^2}{2 \ln(\sigma / \omega_0)^2}, \quad (3)$$

where  $\omega_0$  is the centre frequency of the sinusoid and  $\sigma$  is a scaling factor of the bandwidth.

There are two important characteristics in the Log-Gabor filter. Firstly the Log-Gabor filter function always has zero DC components which contribute to improve the contrast ridges and edges of images. Secondly, the Log-Gabor function has an extended tail at the high frequency end which allows it to encode images more efficiently than the ordinary Gabor function. The Log-Gabor filters have Gaussian transfer functions when viewed on a logarithmic frequency scale instead of a linear one. The constant  $\sigma$ , defines the radial bandwidth  $B$  in octaves,

$$B = 2\sqrt{2/\ln 2} \times \left| \ln\left(\frac{\sigma}{\omega_0}\right) \right|. \quad (4)$$

In this experiment, the ratio  $\sigma / \omega_0$  was kept constant by varying  $\omega_0$  and  $B$  was set to one octave.

## Distance Measure

The Mahalanobis Cosine Distance is used to compute the similarity measure between two Log-Gabor filter banks. Many experimental results have shown that the Mahalanobis Cosine Distance measure provides better performance than many other distance measures [7]. This measure is defined as,

$$D_{MahCoine(u,v)} = - \frac{|m| |n| \cos \theta_{mn}}{|m| |n|} = - \frac{m \cdot n}{|m| |n|}, \quad (5)$$

where  $m$  and  $n$  are two feature vectors transformed into the Mahalanobis space.

## Experimental Result and Discussion

The images are captured by a digital camera under a fluorescent light source. The captured images should be pre-processed before further analysis. Pre-processing includes normalisation illumination, localisation of the solder joint and segmentation. This has been addressed in previous work [10]. The resolution of each solder joint after segmentation is 40 x 40 pixels. Fifty solder joints are used as the training samples and two hundred solder joints are used as the test samples. The solder joint images are divided into five different groups with respect to the amount of solder paste: good, excess, less, bridge and no joint. Other types of defects can be added to the system. In this experiment, the Log-Gabor filter bank is constructed with a total of 5 scales and 6 orientations. 30 sets of coefficients are extracted from the images which contain the significant information for classification. The coefficients are complex by nature, however, the magnitude representation outperforms all others such as real, imaginary and phase representation [11]. For this reason, all coefficients are transformed to magnitude based representation for the next processing step. The similarity score between the train and test image is calculated using the Mahalanobis Cosine Distance.

Detection Error Trade-off (DET) curves can be plotted from the similarity score. Figure 1 shows the DET plot for good joints and defect solder joints and Figure 2 shows the DET plot for good joints and individual defect types. The Equal Error Rate (EER) is the location on the DET curve where the false alarm probability and miss probability are equal. From Figure 2 the EER for the classification of good joints and excess joints is 3% and the good joints and less joints is 4.5%. Again in Figure 1 the EER for the good joints and combination of four defect joints is 2% i.e. the recognition rate for the good joint is 98%. Table 1 is the summarised result for all DET curves in this experiment.

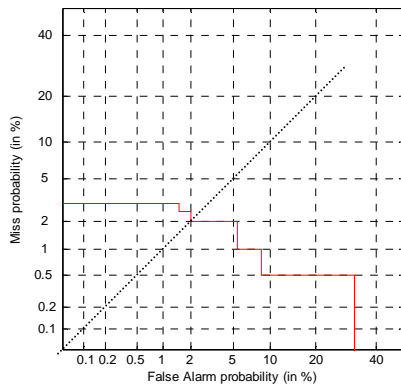


Figure 1. DET curve for classification performance of good joints and defect joints.

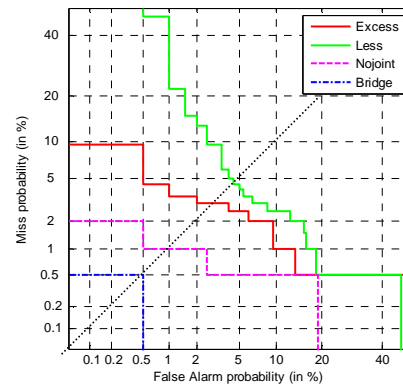


Figure 2. DET curve for classification performance of good joints and individual defect joints.

Solder Joint Types	Classification result (%)				
	G	E	L	N	B
G (Good Joint)	98	3	4.5	1	0.5
E (Excess Joint)	3	97.5	2	3.5	1.5
L (Less Joint)	4.5	2	82.1	50	15
N (No Solder)	1	3	50	85	6
B (Bridge Joint)	0.5	1.5	15	6	94.25

Table 1. Recognition rates for solder joints across five categories.

From the experimental results given in Table 1, the recognition rate of the overall system is 98%. From the first row of Table 1, the detection rate of good joints compared to bridge solder joints and no solder joints is quite high with an EER less than 1%. The EER for the good joint and excess joint is 3%. The system does not perform quite as effectively with good joints and less solder joints. However, the EER is still less than 5%. The error is due to the high degree of similarity between good joints and less solder joints. Table 1 also shows the classification rate among individual defects. This system wrongly classifies some defect joints mostly in less solder joints and no solder joints. From the experimental results, the Gabor filter based solder joint inspection system has a high success rate for automatically classifying solder joints on PCBs.

## Conclusion

In this paper, an investigation into the use of the Log-Gabor filter and the Mahalanobis Cosine Distance measure is applied to the classification of solder joint defects. An Equal Error Rate of 2% was achieved by using a Log-Gabor filter bank. Although the overall recognition rate achieved was 98%, there is still room for improvement. This deficiency can be improved by fusion with other classifier. In general, similar the same techniques can be applied to other object classification tasks such as BGA (Ball Grid Array) inspection, solder paste inspection and IC (Integrated Circuit) lead inspection.

## Reference:

- [1] H. H. Loh and M. S. Lu: Printed circuit board inspection using image analysis, IEEE Transactions on Industry Applications, Vol 35, (1999), p. 426-432.
- [2] B. C. Jiang, C. C. Wang and Y. N. Hsu: Machine vision and background remover-based approach for PCB solder joints inspection, Vol 45, (2007), p. 451-464.
- [3] T. H. Kim, T. H. Cho, Y. S. Moon and S. H. Park: Visual inspection system for the classification of solder joints, Pattern Recognition, Vol 32, (1999), p. 565-575.
- [4] L. Bing, Z. Yun, Y. Guangzhu and Z. Xianshan: ANN Ensembles Based Machine Vision Inspection for Solder Joints, IEEE International Conference on Control and Automation, (2007), p 3111-3115.
- [5] G. Acciani, G. Brunetti and G. Fornarelli: Application of neural networks in optical inspection and classification of solder joints in surface mount technology, IEEE Transactions on Industrial Informatics, Vol 2, (2006), p. 200-209.
- [6] T. Ong, Z. Samad and M. Ratnam: Solder joint inspection with multi-angle imaging and an artificial neural network, The International Journal of Advanced Manufacturing Technology, Vol 38, (2008), p. 455-462.
- [7] J. Cook, C. McCool, V. Chandran and S. Sridharan: Combined 2D/3D Face Recognition Using Log-Gabor Templates, IEEE International Conference on Video and Signal Based Surveillance, AVSS06 (2006), p 83-83.
- [8] J. Daugman: Two-dimensional spectral analysis of cortical receptive field profiles, Vision Research, Vol 20, (1980), p. 847-856.
- [9] D. J. Field: Relations between the statistics of natural images and the response properties of cortical cells, J Opt Soc Am A, Vol 4, (1987), p. 2379-2394.
- [10] N. S. S. Mar, C. Fookes and P. K. D. V. YarLagadda: Design of automatic vision-based inspection system for solder joint segmentation, Achievements in Materials and Manufacturing Engineering, (2009), p 145-151.
- [11] J. Cook, V. Chandran, S. Sridharan and C. Fookes: Gabor Filter Bank Representation for 3D Face Recognition, Digital Image Computing: Techniques and Applications (DICTA05), (2005), p 16-23.